



International Conference on Technologies and Materials for Renewable Energy, Environment and Sustainability, TMREES17, 21-24 April 2017, Beirut Lebanon

## Comparative study on the effect of $\text{NaNO}_2$ in corrosion inhibition of micro-alloyed and API-5L X65 steels in E20 simulated FGE

O.O. Joseph<sup>a,b\*</sup>, S. Sivaprasad<sup>b</sup>, O.S.I. Fayomi<sup>a,c</sup>

<sup>a</sup>Department of Mechanical Engineering, Covenant University, P.M.B. 1023, Ota, Nigeria

<sup>b</sup>Materials Science & Technology Division, CSIR-National Metallurgical Laboratory, Jamshedpur 81007, India

<sup>c</sup>Department of Chemical, Metallurgical & Materials Engineering, Tshwane University of Technology, Pretoria, South Africa

### Abstract

The effect of sodium nitrite ( $\text{NaNO}_2$ ) in the corrosion inhibition of micro-alloyed and API-5L X65 steels in E20 simulated fuel grade ethanol (SFGE) have been investigated via gravimetric method and morphological examination. While  $\text{NaNO}_2$  addition may positively slow down corrosion rate, its concentration within the tested range of 0.2 – 1.0 g/L plays an insignificant role in improving the corrosion resistance of API-5L X65 and micro-alloyed steels. Morphological examination of both steels after immersion tests in the presence and absence of the inhibitor showed pitting corrosion mechanism. Furthermore, statistical analysis confirms with 90 % confidence, that there is no significant difference between the corrosion behaviour of the two steels in E20 SFGE with and without  $\text{NaNO}_2$  inhibitor. Highest protection of the metal surface was achieved at 62.63 % with 0.2 g/L  $\text{NaNO}_2$  for API-5L X65 in E20.

© 2017 The Authors. Published by Elsevier Ltd.

Peer-review under responsibility of the Euro-Mediterranean Institute for Sustainable Development (EUMISD).

**Keywords:**  $\text{NaNO}_2$ ; steels; E20; SFGE; corrosion

\*Corresponding author: Tel.: +234-8035172086

Email address: [funmi.joseph@covenantuniversity.edu.ng](mailto:funmi.joseph@covenantuniversity.edu.ng); [lizajose960@gmail.com](mailto:lizajose960@gmail.com)

## 1. Introduction

Carbon steel, which is commonly used to fabricate storage tanks, pipelines for the transportation of fuel and automobile engine parts & components, is susceptible to corrosion when exposed to fuel grade ethanol (FGE) environment due to the presence of some contaminative constituents (majorly water, chloride and acetic acid) in the fuel [1]. This poses a major problem in the use of existing fuel storage and transportation system for fuel grade ethanol (FGE) as well as in the use of fuel grade ethanol as an alternate fuel for automobile engines.

Among the numerous methods for preventing the degradation of a metallic surface by corrosion, corrosion inhibition is one of the most widely used [2]. Inhibitors are chemically adsorbed on metallic surfaces by forming a protective layer or thin film. Inhibitors can be classified according to their mechanism of action as cathodic, anodic, anodic-cathodic mix or adsorption action. In the case of anodic inhibitor, an important consideration is the inhibitor concentration. Using an inappropriate quantity of inhibitor disturbs the formation of film protection and causes localized corrosion, due to exposed sites on the metal surface.

Anodic inhibitors are thus classified as “dangerous inhibitors”. Examples of anodic inhibitors include orthophosphate, nitrite, ferricyanide, molybdates, nitrates and silicates [2]. The focus of this study is to investigate the effect of sodium nitrite ( $\text{NaNO}_2$ ), a type of anodic inhibitor, in the corrosion inhibition of API-5L X65 and micro-alloyed steels in simulated fuel grade ethanol (SFGE). A Study by [3] have shown that micro-alloyed steel exhibits pitting corrosion when exposed to E20 SFGE due to contamination by chloride. There is significant information in literature on corrosion inhibition of carbon steel with  $\text{NaNO}_2$  in various media [4-8]. However, there is sparse literature regarding the corrosion inhibition of micro-alloyed steels and API-5L X65 steels in E20 SFGE. This work aims to contribute to the body of knowledge in this expanse.

## 2. Experimental

### 2.1. Materials and test environments

Nine samples with dimensions  $30 \times 30 \times 11$  mm each were machined from micro-alloyed steel plates in as-received condition. From an API-5L X65 pipe steel, nine samples with dimensions  $30 \times 30 \times 6$  mm each were equally extracted for mass loss tests and microscopic examination. One of the nine samples from each steel was used for the microscopic test. The chemical composition of API X65 and micro-alloyed steels used in this study include: 0.08 & 0.13 C; 1.22 & 0.77 Mn; 0.25 & 0.01 Si; 0.02 & 0.03 Cr; 0.02 & 0.02 Ni; 0.003 Ti; 0.03 & 0.04 Al; 0.006 & 0.002 Mo; 0.008 & 0.006 Cu; and balance of Fe respectively (all in Wt.%). The microstructures of the as-received steels are shown in Figure 1. The microstructures of the two steels show irregularly dispersed pearlite in a ferrite matrix. The microstructure of X65 steel is expressively finer and more homogenous than that of micro-alloyed steel.

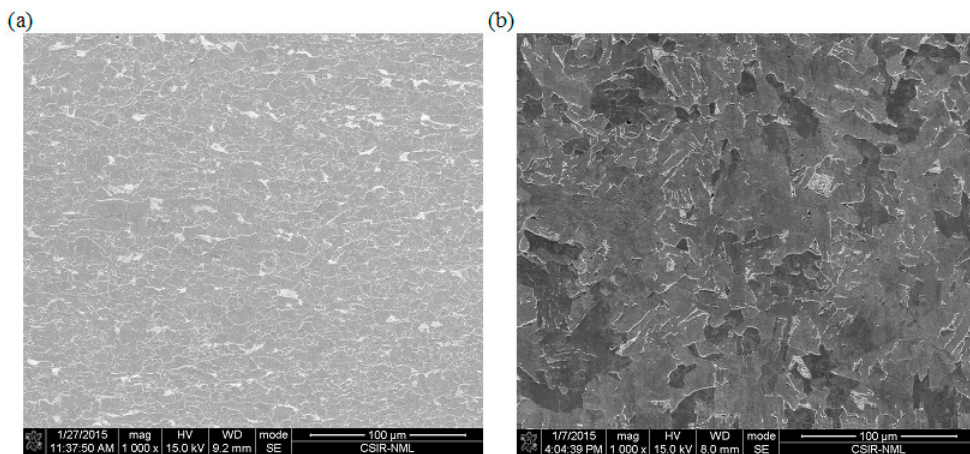


Fig. 1. SEM images at 1000x magnification of as-received (a) API-5L X65 and (b) Micro-alloyed steels.

E20 SFGE environment was prepared following the procedure described in [9] with 98.5 Vol. % ethanol, 0.5 Vol. % pure methanol, 56 mg/L glacial acetic acid, 32 mg/L pure sodium chloride (NaCl), 1 Vol.% ultra-pure water and pure sodium nitrite ( $\text{NaNO}_2$ ) powder (for inhibition). The reagents used were of analar grade.

$\text{NaNO}_2$  is a yellowish-white crystalline solid with 68.995 g/mol molecular weight. The two-dimensional structure of  $\text{NaNO}_2$  is shown in Figure 2. To determine the role of  $\text{NaNO}_2$  concentration in the inhibition behaviour, concentrations of 0.2, 0.6 and 1 g/l were used for the corrosion tests. Control tests were carried out in the absence of the inhibitor.

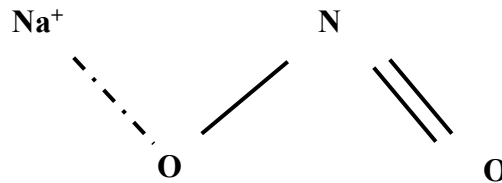


Fig. 2. Two-dimensional structure of  $\text{NaNO}_2$ .

## 2.2. Immersion tests

Eight samples each from micro-alloyed and API-5L X65 steels were dry-abraded with silicon carbide paper grades of 80, 180, 320, 600 and 800 microns for the immersion tests. The abraded samples were degreased with acetone and initial weight was measured. The immersion tests were carried out for a duration of 60 days at ambient temperature of 27°C. The samples were suspended in sealed 300 ml plastic containers, carrying 200 ml of the test solution. Each test was replicated to determine the reproducibility of the tests. At the end of the exposure period, the samples were removed from the test solution, dried and cleaned following the chemical cleaning procedure described in [3,9]. Final weight measurements were taken and corrosion rate in mils per year (mpy) calculated with the relation given in Equation (1) [9].

$$C.R. = K \times W / A \times T \times D \quad (1)$$

Where C.R. is corrosion rate (mpy), K is a constant (534), W is the mass loss (mg), A is the sample area ( $\text{in}^2$ ), T is the exposure time (hours) and D is density ( $\text{g/cm}^3$ ). The inhibitor efficiency ( $E_f$ ) was computed as shown in Equation (2) [2].

$$E_f = \frac{R_i - R_o}{R_o} \times 100 \quad (2)$$

Where  $R_i$  the corrosion rate of metal with inhibitor,  $R_o$  is corrosion rate of metal without inhibitor, and  $E_f$  is inhibitor efficiency (percentage).

Morphological changes in the tested samples were also examined using a JEOL Scanning electron microscope, Model number JSM 840A.

## 3. Results and Discussion

Figure 3 shows the variation of corrosion rates with  $\text{NaNO}_2$  concentration obtained after immersion tests for micro-alloyed and API-5L X65 steels. In general, the X65 steel exhibited higher corrosion rates than micro-alloyed

steel which indicates that anodic reactions are more spontaneous in X65 steel. Highest corrosion rates of  $1.31 \times 10^{-3}$  and  $1.25 \times 10^{-3}$  mpy were obtained for X65 and micro-alloyed steels in the control tests. However, the two steels responded differently to variations in  $\text{NaNO}_2$  concentration. Corrosion rate of X65 steel increased with increase in  $\text{NaNO}_2$  concentration while that of micro-alloyed steel decreased. Significant protection was achieved on X65 steel at 0.2 g/L  $\text{NaNO}_2$ , the lowest concentration with respect to the control test. Corrosion rate of  $4.90 \times 10^{-4}$  mpy was obtained which is approximately 62 % lower than the control test value. This suggests that  $\text{NaNO}_2$  is best effective at inhibiting fuel ethanol corrosion of API-5L X65 steel at low concentrations. Higher concentrations of the chemical resulted in higher corrosion rates of  $1.11 \times 10^{-3}$  and  $1.12 \times 10^{-3}$  mpy for samples tested in 0.6 and 1 g/L  $\text{NaNO}_2$  respectively, though these values are lower in comparison to the control test result.

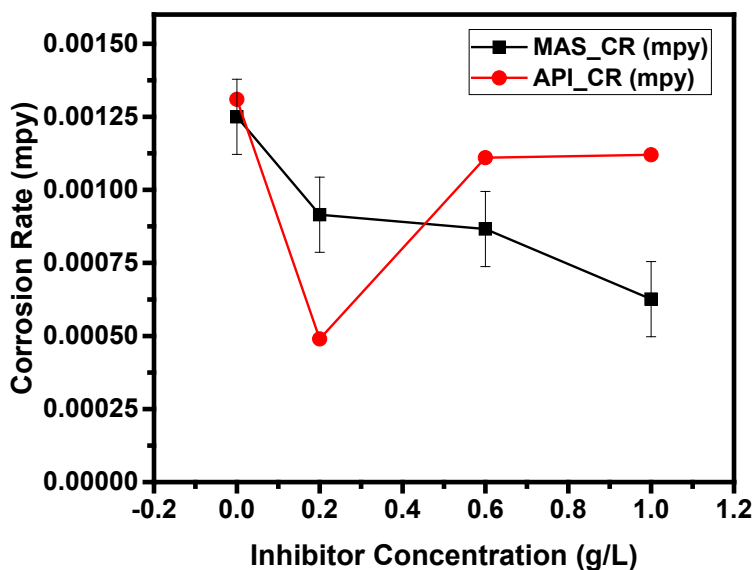


Fig. 3. Variation of corrosion rate with inhibitor concentration for API-5L X65 and Micro-alloyed steels.

Conversely, the corrosion rate of micro-alloyed steel followed a decreasing trend with increasing concentration of  $\text{NaNO}_2$ . Best protection of  $6.26 \times 10^{-4}$  mpy was achieved at 1 g/L  $\text{NaNO}_2$ . A comparison of the degradation behaviour of the two steels in the presence of  $\text{NaNO}_2$  shows that micro-alloyed steel is more responsive to the protective action of the adsorbent species present in  $\text{NaNO}_2$ . However, within the limits of  $\text{NaNO}_2$  concentrations used for this study, the lowest corrosion rate overall was achieved by X65 steel with smallest inhibitor concentration of 0.2 g/L.

The statistical significance of the experimental data obtained was further investigated with the aim of determining if the effect of varying the concentration of  $\text{NaNO}_2$  was significant. Two-factor Analysis of variance (ANOVA) test was used to determine the statistical significance of the functional variables. Table 1 shows the results of the ANOVA test. Based on the determined mean square ratio, it can be concluded with 90 % confidence that inhibitor concentration had no significant effect on the mass loss of the two steels. Furthermore, it can also be concluded at the same confidence level, that there is no significant difference between the behaviour of API-5L X65 steel and micro-alloyed steel in E20 with and without  $\text{NaNO}_2$  inhibitor additions.

Figure 4 shows the variation of inhibitor efficiency with inhibitor concentration for both X65 and micro-alloyed steels. As indicated by the corrosion rates, inhibitor efficiency decreased with increase in  $\text{NaNO}_2$  concentration for X65 steel, while increase was noted for micro-alloyed steel. X65 steel exhibited highest inhibitor efficiency of 62.63 % with 0.2 g/L  $\text{NaNO}_2$  in simulated E20 while micro-alloyed steel had its highest value of 49.93 % with 1 g/L  $\text{NaNO}_2$ .

Table 1. ANOVA test results for the API-5L X65 and micro-alloyed steel mass loss data

Source of Variation	Sum of Squares (SS)	Degrees of Freedom (DF)	Mean Square (MS)	Mean Square Ratio (MSR)	Minimum MSR at 90% confidence
Inhibitor Concentration	0.0293	3	0.0098	1.44	5.39
Metal Type	0.0045	1	0.0045	0.66	5.54
Residual	0.0204	3	0.0068		
Total	0.0541	7			

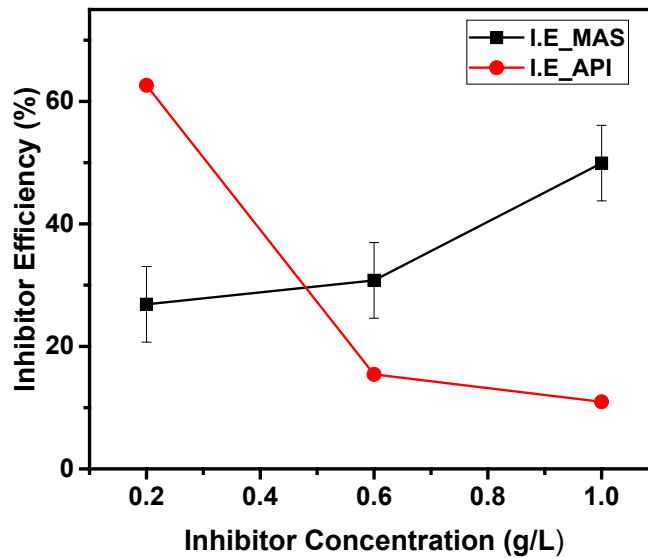


Fig. 4. Variation of inhibitor efficiency with inhibitor concentration for API X65 and Micro-alloyed steels.

The phenomenon of molecular adsorption was further used to clarify the corrosion inhibition mechanism of  $\text{NaNO}_2$  on API-5L X65 and micro-alloyed steel. The likely mode of adsorption was determined by testing the experimental data with various adsorption isotherms. Adsorption isotherms supply information on the inhibitor molecular behaviour and its interaction with the metal surface [10]. In addition, the standard free energy of adsorption was evaluated with the relation given in Equation (3) [11].

$$k = \frac{1}{55.5} \exp\left(-\frac{\Delta G^o_{ads}}{RT}\right) \quad (3)$$

Where  $\Delta G^o_{ads}$  is the standard free energy of adsorption,

$R$  = molar gas constant and

$T$  = absolute temperature.

Table 2 shows the thermodynamic parameters obtained for API-5L X65 and micro-alloyed steel in E20 simulated FGE with NaNO<sub>2</sub> inhibitor. The negative values of ΔG<sup>o</sup><sub>ads</sub> indicate that the adsorption is spontaneous. ΔG<sup>o</sup><sub>ads</sub> obtained for NaNO<sub>2</sub> inhibitor concentrations of 0.2, 0.6 and 1 g/L was within the range of -11 to -22 kJ/mol, indicating physisorption mode of adsorption. ΔG<sup>o</sup><sub>ads</sub> values that are -20 kJ/mol and less negative are consistent with physical adsorption which involves an electrostatic interaction between charged atoms and the charged metal [12,13]. The data was further fitted with Langmuir, Freundlich and Temkin adsorption isotherms. Figure 5 shows the best fit obtained for the data with the Temkin isotherm which is given by Equation (4) [14]. The Temkin adsorption isotherm assumes the heat of adsorption of the NaNO<sub>2</sub> ions decreases linearly with increasing coverage. A regression coefficient of 0.956 was obtained.

$$\Delta H_{ad} = \Delta H_{ad}^0 (1 - \alpha_T \theta) \tag{4}$$

Table 2. Thermodynamic parameters for API-5L X65 and Micro-alloyed steel in E20 with NaNO<sub>2</sub> inhibitor

Inhibitor concentration	Θ	K	log K	1-Θ	Θ/1-Θ	ΔG (kJ/mol-1)
Control	0.00	0.00	0.00	1.00	0.00	0.00
0.2 g/L NaNO <sub>2</sub>	0.63	8378.00	3.92	0.37	1.68	-22.38
0.6 g/L NaNO <sub>2</sub>	0.13	240.25	2.38	0.87	0.14	-13.58
1.0 g/L NaNO <sub>2</sub>	0.08	85.78	1.93	0.92	0.09	-11.03

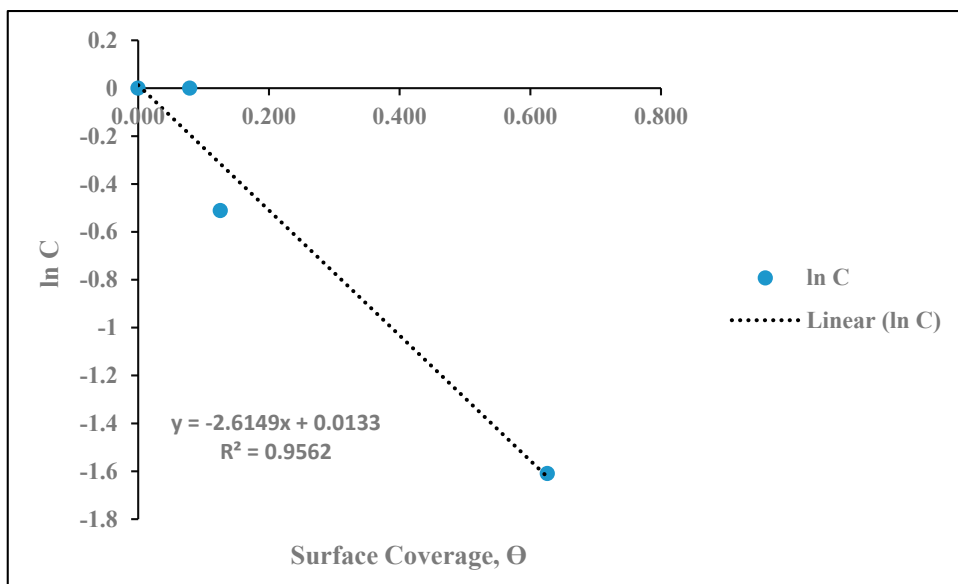


Fig. 5. Variation of inhibitor concentration, ln C with surface coverage, Θ for API X65 and Micro-alloyed steels.

Figure 6 shows the morphology of API-5L X65 and micro-alloyed steel after the control tests. Degradation of the samples was by pitting corrosion. The arrows point to the pits. A comparison of the severely pitted surface of API-5L X65 steel with the fewer pits on micro-alloyed steel confirms the mass loss results where API-5L X65 was seen to exhibit higher corrosion rates than micro-alloyed steel.

Figure 7 shows the typical SEM images obtained for micro-alloyed steel samples tested in E20 with 0.2 and 0.6 g/L NaNO<sub>2</sub> inhibitor. The corrosion mechanism portrays a combination of uniform and pitting corrosion. Uniform corrosion can be seen in the general anodic dissolution of the metal surface. The arrows depicts the pits. Similar corrosion mechanism of pitting was observed on the control test samples, though there is apparent reduction in the



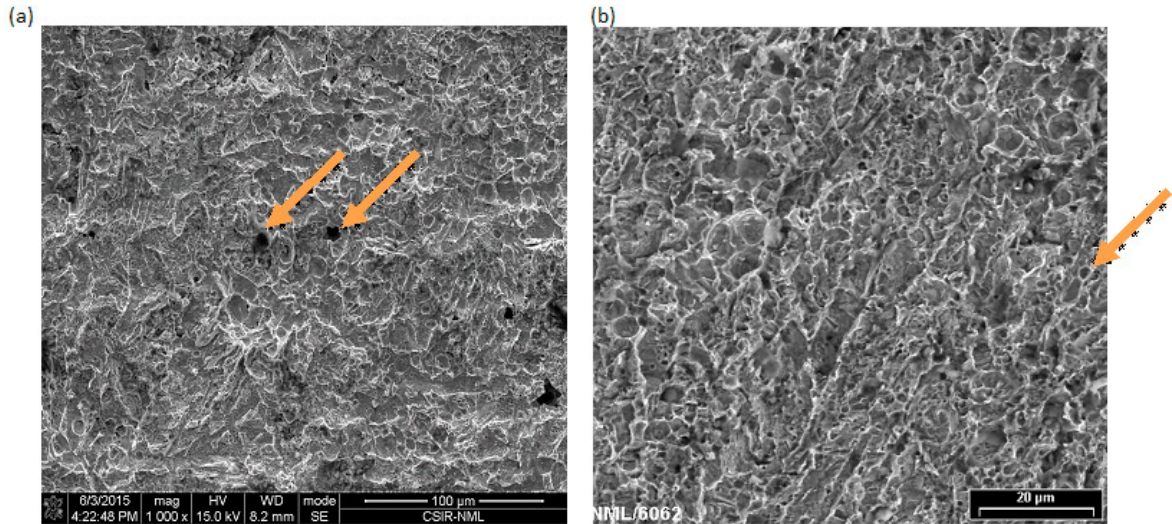


Fig. 6. SEM images showing pitting corrosion of (a) Micro-alloy and (b) API-5L X65 steels in E20 SFGE without inhibitor.

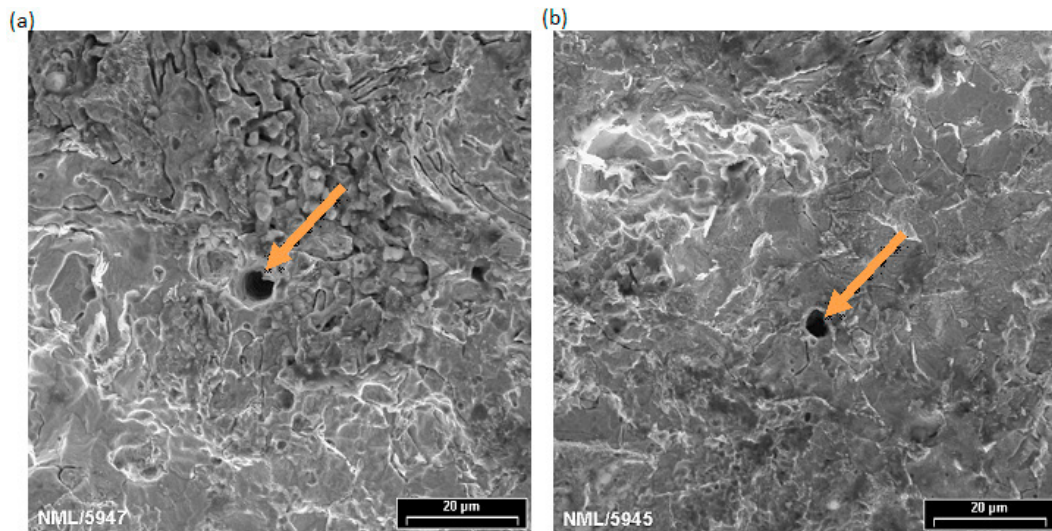


Fig. 7. SEM images showing pitting corrosion of micro-alloyed steel in (a) E20 with 0.2 g/L NaNO<sub>2</sub> and (b) E20 with 0.6 g/L NaNO<sub>2</sub>. Arrows point to pits.

density of the pits. The morphological examination results in Figure 7 confirms the insignificant effect of NaNO<sub>2</sub> inhibitor in corrosion rate reduction.

## Conclusion

The effect of NaNO<sub>2</sub> concentration on the degradation of API-5L X65 and micro-alloyed steels have been investigated. Highest inhibitor efficiency was obtained with 0.2 g/L NaNO<sub>2</sub> on X65 steel. Slightly improved corrosion resistance with increase in NaNO<sub>2</sub> concentration was observed only on micro-alloyed steel. Statistical analysis confirmed that inhibitor concentration had an insignificant effect on mass loss of the steels. In addition, there is no significant difference between the degradation behaviour of the two steels with and without NaNO<sub>2</sub>

inhibitor. Thermodynamic evaluation of  $\text{NaNO}_2$  on the steels confirm physisorption mode of adsorption obeying the Temkin adsorption isotherm.

## References

- [1] Cao L, Frankel GS, Sridhar N. Effect of chloride on stress corrosion cracking susceptibility of carbon steel in simulated fuel grade ethanol. *Electrochim Acta*, 2013; 104: 255–266.
- [2] Camila GD, Alexandre FG. Corrosion inhibitors-principles, mechanisms and applications. In: Aliofkhaezrai M, editor. *Developments in corrosion protection*. Croatia: InTech; 2014. p. 365-379.
- [3] Joseph OO, Loto CA, Sivaprasad S, Ajayi JA, Fayomi OSI. Comparative assessment of the degradation mechanism of micro-alloyed steel in E20 and E80 simulated fuel grade ethanol environments. *AIP Conference Proceedings*, 2016; 1758: 020019.
- [4] Kahraman R, Saricimen H, Al-Zahrani M. Effect of inhibitor treatment on corrosion of steel in a salt solution. *J Mat Eng Perf*, 2003; 12: 524-528.
- [5] Gaius DE, Geoffrey W, Willem D, Jennifer M. The synergistic effect of iodide and sodium nitrite on the corrosion inhibition of mild steel in Bicarbonate–Chloride Solution. *Materials*, 2016; 9: 868.
- [6] Karim S, Mustafa CM, Assaduzzaman Md, Islam M. Effect of nitrite ion on corrosion inhibition of mild steel in simulated cooling water. *Chem Eng Res Bull*, 2010; 14: 87-91.
- [7] Girčienė O, Ramanauskas R, Gudavičiūtė L, Martušienė A. Inhibition effect of sodium nitrite and silicate on carbon steel corrosion in chloride-contaminated alkaline solutions. *Corrosion*, 2011; 67:125001-1-125001-12.
- [8] Maan H, Shatha AS, Adeeb H, Inas MA. Utilizing of Sodium Nitrite as Inhibitor for Protection of Carbon Steel in Salt Solution. *Int J Electrochem Sci*, 2012; 7: 6941-6950.
- [9] Joseph OO, Loto CA, Sivaprasad S, Ajayi JA, Tarafder S. Role of chloride in the corrosion and fracture behavior of micro-alloyed steel in E80 simulated fuel grade ethanol environment. *Materials*, 2016; 9: 463.
- [10] Loto RT, Loto CA, Joseph O, Gabriel O. Adsorption and corrosion inhibition properties of thiocarbonyl on the electrochemical behavior of high carbon steel in dilute acid solutions. *RINP*, 2016; 6: 305-314.
- [11] Loto CA, Joseph OO, Loto RT. Adsorption and inhibitive properties of camellia sinensis for aluminium alloy in HCl. *Int J Electrochem Sci*, 2014; 3637-3649.
- [12] Nnanna AL, Nwadiuko CO, Ekekwe DN, Ukpabi FC, Udensi CS, Okeoma BK, Onwuagba NB, Mejeha MI. *Amer J Mater Sci*, 2011; 1: 143-14
- [13] Alaneme KK, Olusegun SJ. Corrosion inhibition performance of lignin extract of sun flower (*Tithonia diversifolia*) on medium carbon low alloy steel immersed in  $\text{H}_2\text{SO}_4$  solution. *Leo J Sci*, 2012; 20: 59-70.
- [14] Kim KT, Kim HW, Chang HY, Lim BT, Park HB, Kim YS. Corrosion inhibiting mechanism of nitrite ion on the passivation of carbon steel and ductile cast iron for nuclear power plants. *Adv Mat Sci Eng*, 2015; 408138: 1-16.